J Electroceram (2006) 16:343–346
DOI 10.1007/s10832-006-9876-2

Microstructural and dielectric studies of *A*-site calcium doped $PbZr_{0.94}Ti_{0.06}O_3$ ceramics

Haitao Huang · Li Min Zhou · Ling Bing Kong

Abstract The microstructure-property relationship of calcium doped $PbZr_{0.94}Ti_{0.06}O_3$ (PZT 94/6) ceramics has been studied. It was found that calcium doping on the *A*-site turns the ferroelectric PZT 94/6 into antiferroelectric. $\frac{1}{2}\{hk0\}$ superlattice reflections were observed in the selected area diffraction pattern (SADP) of PZT 94/6 which indicated an in-phase oxygen octahedra tilting in the ferroelectric PZT 94/6. When 4 mol% of calcium was added as a dopant, the material became antiferroelectric at room temperature, with the characteristic $\frac{1}{4}\{hk0\}$ superlattice reflections observed in the SADP. The *P*-*E* hysteresis loop measurement also supports this conclusion. As the temperature increased, an *AFE-FE* phase transition occurred and this was accompanied by a hunch-like dielectric anomaly at around 140°C.

Keywords PZT · Ferroelectrics · Antiferroelectrics · TEM · Phase transition

1 Introduction

Since the discovery of perovskite ferroelectrics, the solid solution of $PbZrO_3$-$PbTiO_3$ (PZT) system has attracted intensive studies due to its excellent technical properties, such as pyro- and piezo-electricity. The PZT solid solution displays a complex phase diagram [1]. At room temperature, depending on the Zr/Ti ratio, it can exist in an antiferroelectric (*AFE*) orthorhombic phase A_O, a ferroelectric (*FE*) rhombohedral phase F_R (which can be further divided into a high temperature $F_{R(HT)}$ phase and a low temperature $F_{R(LT)}$ phase), a ferroelectric tetragonal phase F_T, or a ferroelectric monoclinic phase [2]. For piezoelectric applications, the composition near the morphotropic phase boundary is usually selected; while for the pyroelectric applications, a composition near the antiferroelectric and ferroelectric phase boundary is chosen [3].

An attractive feature of PZT is that its properties can be easily tailored by various dopants on either the *A*- or *B*-sites of the ABO_3 perovskite structure. For example, Ca^{2+}, Ba^{2+}, Sr^{2+}, and La^{3+}, etc. can be doped on the *A*-site and Sn^{4+}, Ce^{4+}, Fe^{3+}, and Nb^{5+}, etc. can be doped on the *B*-site [1, 4–6]. It has been shown that for Zr-rich PZT, a small amount of doping of calcium on the *A*-site increases the pyroelectric coefficient and decreases the dielectric constant [7]. A dielectric anomaly has been observed in the permittivity curve at a temperature of ∼140°C. This anomaly corresponds to an *AFE-FE* phase transition. How the properties are related to the microstructure of the material has not yet been studied. In general, the change in physical properties can be predicted from the structural change of the material. It is agreed that in perovskites, numerous structural distortions can occur to the three-dimensional corner-linked BO_6 octahedra and/or the *A*-site cations. The cation displacement has some relation with the oxygen octahedra tilting [8]. Since ferroelectricity or antiferroelectricity are directly related to the displacements of cations, microstructural studies by transmission electron microscope (TEM) can thus reveal the

H. Huang (✉)
Department of Applied Physics, The Hong Kong Polytechnic University, Hung Hom, Kowloon, Hong Kong
e-mail: aphhuang@polyu.edu.hk

L. M. Zhou
Department of Mechanical Engineering, The Hong Kong Polytechnic University, Hung Hom, Kowloon, Hong Kong

L. B. Kong
Temasek Lab, National University of Singapore, 10 Kent Ridge Crescent, Singapore 119260

structure-property relationships of doped PZT. The purpose of this paper is to study the microstructure of calcium doped PZT and its relation with the dielectric and ferroelectric properties.

2 Experiments

The materials were made from mixed oxide powders by a conventional solid-state reaction method. The starting powders were high purity PbO (>99%, Fluka), ZrO_2 (>99%, Aldrich), TiO_2 (>99%, Merck) and $CaCO_3$ (>99%, Fluka). These constituents were weighed accurately according to the chemical formula of $(Pb_{1-x}Ca_x)(Zr_{0.94}Ti_{0.06})O_3$ (short for PCZT $100x/94/6$), where $x = 0$ and 0.04. All the grinding and ball milling were done using a ZrO_2 grinding media. The mixed powders were calcined and sintered at 880°C and 1200°C, respectively. Before sintering, the powders were uniaxially cold pressed into pellets at 200 MPa using 1.5 wt.% polyvinyl alcohol (PVA) as a binder. The pressed green samples with a diameter of 25 mm and a thickness of 2.5 mm were then sintered in double closed alumina crucibles under a PbO atmosphere. A high heating rate was adopted in order to suppress the unwanted pyrochlore phase. Details of the processing can also be found in [7].

The temperature dependence of the low field dielectric constant was measured using a precision LCR meter (HP4284A). The sample used for dielectric measurement was electroded with silver paste to form a parallel-plate-capacitor and was uniformly heated in a three-zone tube furnace. The measurement frequencies were 1, 10, 100, and 1000 kHz, respectively. The polarization-electric field (P-E) behavior was characterized by means of a ferroelectric tester (RT6000, Radiant Technology). The TEM studies were done on a 200 kV JEOL JEM-2010 microscope equipped with a double-tilt stage. The detailed procedure for TEM sample preparation can be found elsewhere [8].

3 Results and discussions

The temperature dependence of the dielectric constant of Ca-doped PZT 94/6 is shown in Fig. 1. A dielectric maximum, which corresponds to the *FE-PE* phase transition, can be clearly seen at a temperature of ~230°C. Both the transition temperature and the maximum dielectric constant decrease with the calcium doping. A hunch-like dielectric anomaly (indicated as the minor peak by an arrow in Fig. 1(b)) is observed at a lower temperature. This dielectric anomaly corresponds to an *AFE-FE* phase transition. This sudden jump in dielectric constant is indicative of a first order phase transition. A large temperature hysteresis (inset of Fig. 1(b)) can be observed around this dielectric anomaly,

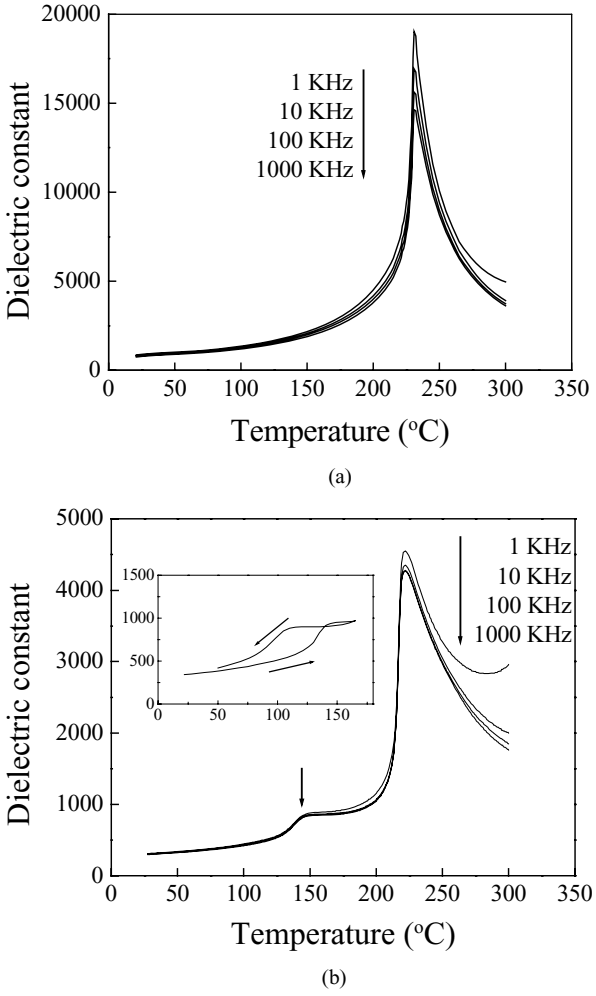

Fig. 1 Temperature dependence of dielectric constant of (a) PCZT 0/94/6 and (b) PCZT 4/94/6

which further confirms that the phase transition is the first order. The *AFE-FE* phase transition cannot be found to be a diffuse one within the measuring frequencies from 1 kHz to 1 MHz though it has been reported that the *AFE-FE* transition in PZT 95/5 is quite diffused [9].

Both the reciprocal dielectric constants of PCZT 0/94/6 and PCZT 4/94/6 ceramics accurately fit the Curie-Weiss law above the Curie temperature,

$$\frac{1}{\varepsilon} = \frac{T - T_0}{C} \tag{1}$$

where ε is the dielectric constant, T is temperature, T_0 is the Curie point, and C is the Curie-Weiss constant. The Curie-Weiss constant calculated at 10 kHz is about 3.4×10^5 K, a little bit higher than the value obtained by the Landau phenomenological theory, which is about 2×10^5 K [10]. Below the Curie point, the reciprocal dielectric constant also fits to the Curie-Weiss law but with a different slope.

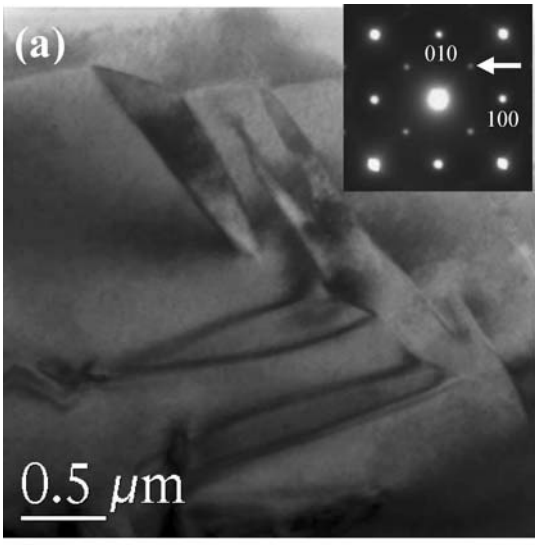

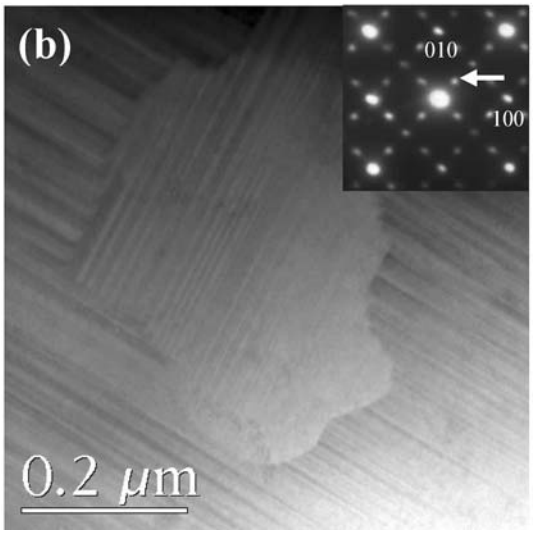

Fig. 2 Domain patterns of (a) PCZT 0/94/6 and (b) PCZT 4/94/6. The insets are the SADPs viewed along the [001] zone axis. The $\frac{1}{2}\{hk0\}$ and $\frac{1}{4}\{hk0\}$ superlattice reflections are indicated by an arrow in the insets of (a) and (b), respectively

The domain patterns of PCZT 0/94/6 and PCZT 4/94/6 ceramics are shown in Fig. 2. Wedge-shaped domains are observed in PCZT 0/94/6. Similar patterns have been reported by other researchers [11]. Antiferroelectric domains, which have irregular shapes, are observed in the PCZT 4/94/6 ceramic sample. Perpendicular streaks of lines indict that the antiferroelectric domains have 90° boundaries (Fig. 2(b)). Similar 90° domain walls have been observed in our previous work in cerium-doped PZT ceramics [8].

The selected area diffraction patterns (SADPs) of the domain viewed along [001] zone axis are shown as insets of Fig. 2. It is generally agreed that at room temperature the rhombohedral $F_{R(LT)}$ phase exhibits both the cation shift along the pseudo-cubic [111] direction and the oxygen octahedra tilting around this direction [12]. The oxygen octahedron tilting is a result of the optical phonon mode condensation at either the R or M point of the Brillouin zone boundary [13]. The tilting of one octahedron around the principle axis will cause the antiparallel tilting of all the neighboring octahedra lying in the same plane perpendicular to that axis. This doubles the unit cell in that plane. The $\frac{1}{2}\{hk0\}$ superlattice reflections observed in PCZT 0/94/6 result from this in-phase tilting of oxygen octahedra. In contrast for the PCZT 0/90/10 sample, which has anti-phase tilting of the oxygen octahedra, only $\frac{1}{2}\{hkl\}$ superlattice reflections (the so-called F spots) can be observed [14].

For the PCZT 4/94/6 sample, $\frac{1}{4}\{hk0\}$ superlattice reflections are observed as shown in the inset of Fig. 2(b). This is indicative of an antiferroelectric phase. Antiferroelectricity in the PZT system is a result of the condensation of the Σ_3 phonon mode [13]. The Σ_3 mode contains the antiparallel

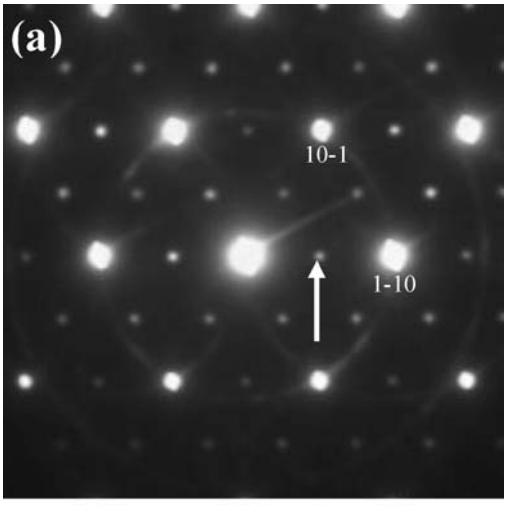

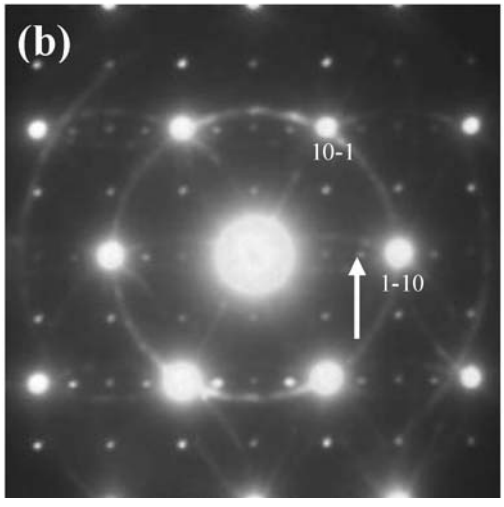

Fig. 3 SADPs of (a) PCZT 0/94/6 and (b) PCZT 4/94/6 viewed along the [111] zone axis. The $\frac{1}{2}\{hk0\}$ and $\frac{1}{4}\{hk0\}$ superlattice reflections are indicated by an arrow in (a) and (b), respectively

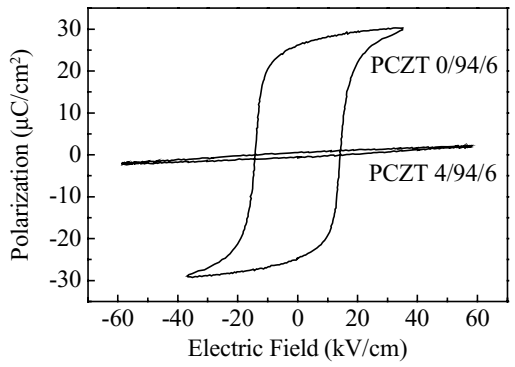

Fig. 4 *P-E* hysteresis loop of Ca-doped PZT

displacements of Pb^{2+} along the (001) surface diagonals of the parent cubic perovskite structure. Due to the antipolar movements of the Pb^{2+} ions, a unit cell with a size of $2\sqrt{2}a \times 2\sqrt{2}a$ (a being the lattice parameter of the pseudocubic) is formed in the (001) plane [8] and this results in the appearance of the $\frac{1}{4}\{hk0\}$ superlattice reflections. Within one single antiferroelectric domain, however, only one set of the $\frac{1}{4}\{hk0\}$ superlattice reflections with either $hk > 0$ or $hk < 0$ can be observed. In the inset of Fig. 2(b), both sets of the $\frac{1}{4}\{hk0\}$ superlattice reflections are observed which means that the antipolar movements of the Pb^{2+} ions in the two neighboring domains are perpendicular to each other. Hence the observed domains form a 90° boundary.

Figure 3 shows the [111] SADPs of PCZT ceramics. Indexing of the reflections is done according to the pseudocubic parent perovskite structure. $\frac{1}{2}\{hk0\}$ superlattice reflections can be observed in PCZT 0/94/6 due to the in-phase tilting of oxygen octahedra. In contrast, $\frac{1}{4}\{hk0\}$ superlattice reflections are observed in PCZT 4/94/6 due to the antipolar displacements of Pb^{2+} ions. The *P-E* hysteresis loop in Fig. 4 clearly indicates that PCZT 0/94-6 is ferroelectric while PCZT 4/94/6 is antiferroelectric. The double-hysteresis loop, which is commonly observed for antiferroelectrics, cannot be seen due to the very high *AFE-FE* transition field in this kind of material. The ceramics is electrically broken down before the *AFE-FE* transition field is reached.

4 Conclusions

The dielectric properties and microstructures of calcium doped PZT have been studied. It was found that PCZT 0/94/6 is ferroelectric. $\frac{1}{2}\{hk0\}$ superlattice reflections were observed in the SADP, which is indicative of an in-phase oxygen octahedra tilting in PCZT 0/94/6. When 4 mol% of calcium is doped on the *A*-site, the material becomes antiferroelectric at room temperature with $\frac{1}{4}\{hk0\}$ superlattice reflections observed in the SADP. The *P-E* hysteresis loop measurement confirms this conclusion. As the temperature is increased, an *AFE-FE* phase transition occurs and this is accompanied by a hunch-like dielectric anomaly at around 140°C.

Acknowledgments The authors are grateful to financial supports from the Hong Kong Polytechnic University (Grant No.: G-YX09) and the Research Grant Council of HKSAR (Grant No.: PolyU 5279/04E).

References

1. B. Jaffe, W.R. Cook, and H. Jaffe, *Piezoelectric Ceramics* (Academic Press, London, 1971).
2. B. Noheda, D.E. Cox, G. Shirane, J.A. Gonzalo, L.E. Cross, and S.-E. Park, *Appl. Phys. Lett.*, **74**, 2059 (1999).
3. M.H. Lee, R. Guo, and A.S. Bhalla, *J. Electroceram.*, **2**, 229 (1998).
4. R.E. Newnham, *MRS Bull.*, **22**(5), 20 (1997).
5. G.H. Haertling, *J. Am. Ceram. Soc.*, **82**, 797 (1999).
6. N. Setter and R. Waser, *Acta Mater.*, **48**, 151 (2000).
7. H. Huang, Z. Tianshu, J.T. Oh, and P. Hing, *Ferroelectrics*, **274**, 55 (2002).
8. H. Huang, J. Guo, L.B. Kong, H.H. Hng, J.T. Oh, P. Hing, and O.K. Tan, *Solid State Commun.*, **125**, 297 (2003).
9. Y.I. Wang, Z.M. Cheng, Y.R. Sun, and X.H. Dai, *Physica B*, **150**, 168 (1988).
10. H. Huang, C.Q. Sun, Z. Tianshu, and P. Hing, *Phys. Rev. B*, **63**, 184112 (2001).
11. J. Ricote, R.W. Whatmoew, and D.J. Barber, *J. Phys.: Condens. Matter*, **12**, 323 (2000).
12. A.M. Glazer, S.A. Mabud, and R. Clarke, *Acta Crystallogr. Sect. B: Struct. Crystallogr. Cryst. Chem.*, **34**, 1060 (1978).
13. D. Viehland, *Phys. Rev. B*, **52**, 778 (1995).
14. H. Huang, L.M. Zhou, J. Guo, H.H. Hng, J.T. Oh, and P. Hing, *Appl. Phys. Lett.*, **83**, 3692 (2003).